

Silicone Surface with Drug Nanodepots for Medical Devices

Jiratchaya Mokkaphan,[†] Wijit Banlunara,[‡] Tanapat Palaga,^{§,#} Premsuda Sombuntham,^{||} and Supason Wanichwecharungruang^{*,†,‡,#}

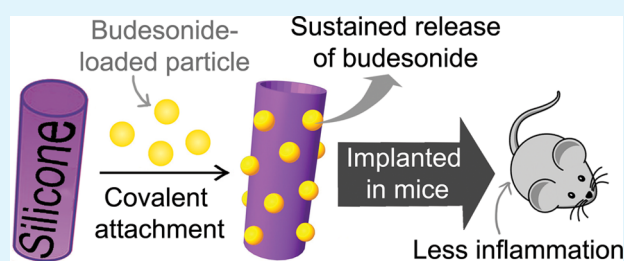
[†]Program of Petrochemical and Polymer Science, Faculty of Science, [‡]Department of Pathology, Faculty of Veterinary Science, [§]Department of Microbiology, Faculty of Science, ^{||}Department of Otolaryngology Head and Neck Surgery, Faculty of Medicine, [†]Department of Chemistry, Faculty of Science, and [#]Nanotec-CU Center of Excellence on Food and Agriculture, Chulalongkorn University, Bangkok 10330, Thailand

Supporting Information

ABSTRACT: An ideal surface of poly(dimethylsiloxane) (PDMS) medical devices requires sustained drug release to combat various tissue responses and infection. At present, a noncovalent surface coating with drug molecules using binders possesses a detachment problem, while covalently linking drug molecules to the surface provides no releasable drug. Here, a platform that allows the deposition of diverse drugs onto the PDMS surface in an adequate quantity with reliable attachment and a sustained-release character is demonstrated. First, a PDMS surface with carboxyl functionality (PDMS-COOH) is generated

by subjecting a PDMS piece to an oxygen plasma treatment to obtain silanol moieties on its surface, then condensing the silanols with (3-aminopropyl)triethoxysilane molecules to generate amino groups, and finally reacting the amino groups with succinic anhydride. The drug-loaded carriers with hydroxyl groups on their surface can then be esterified to PDMS-COOH, resulting in a PDMS surface covalently grafted with drug-filled nanocarriers so that the drugs inside the securely grafted carriers can be released. Demonstrated here is the covalent linking of the surface of a PDMS endotracheal tube with budesonide-loaded ethylcellulose nanoparticles. A secure and high drug accumulation at the surface of the tubes (0.025 mg/cm²) can be achieved without changes in its bulk property such as hardness (Shore-A), and sustained release of budesonide with a high release flux during the first week followed by a reduced release flux over the subsequent 3 weeks can be obtained. In addition, the grafted tube possesses more hydrophilic surface and thus is more tissue-compatible. The grafted PDMS pieces show a reduced in vitro inflammation in cell culture and a lower level of in vivo tissue responses, including a reduced level of inflammation, compared to the unmodified PDMS pieces, when implanted in rats. Although demonstrated with budesonide and a PDMS endotracheal tube, this platform of grafting a PDMS surface with drug-loaded particles can be applied to other drugs and other devices.

KEYWORDS: silicone surface, drug release, surface functionalization, inflammation, implantation, endotracheal tube



INTRODUCTION

Because its ease of fabrication (ease of cross-linking), biocompatibility, and advantageous chemical (bioinertness and oxidative and thermal stability) and physical (optical transparency and adjustable modulus) characteristics, poly-(dimethylsiloxane) (PDMS) is a popular thermosetting silicone elastomer used for the production of medical devices to be put inside the body, either temporarily or permanently, such as catheters, artificial prosthetics, and subcutaneous sensors. Nevertheless, inflammation and infection occur frequently at the tissues surrounding the devices.^{1–4} The hydrophobic nature of the PDMS surface contributes greatly to the formation of a dead-space between the hydrophilic tissue and the implanted devices, resulting in the colonization of microorganisms and the formation of biofilms.^{5,6} Moreover, the low surface free energy of PDMS imparts a poor wettability to the material, which results in tissue irritation, abrasion, and ulceration.^{7,8} In fact, the surface wettability directly influences the interaction between tissue cells and surfaces and is, therefore, one of the first

concerns in the development of new devices for biomedical applications.⁹ This factor is critically important for percutaneous devices, which pass through the skin from the outside to the interior of the body, because bacteria can enter the body along the device surface.

The problems of the hydrophobic surface of PDMS, together with its frequent infection and inflammation after being implanted, need to be solved without altering the excellent bulk properties of the material. Various surface functionalization strategies have been carried out to make the PDMS surface more hydrophilic or even charged, but infection and inflammation still occur.^{10–13} Coating the surface of PDMS medical devices with drug molecules, using various noncovalent interactions and binders, to give the devices a drug-release character¹⁴ has resulted in peel-off and drug migration

Received: August 26, 2014

Accepted: October 14, 2014

Published: October 14, 2014

problems with no significant improvement compared to the uncoated devices.¹⁵ Covalent linking of drug molecules to the surface is another approach to lessen the infection, inflammation, and tissue reaction levels.^{16–18} However, in addition to a low drug content on the surface, another limitation of this approach is that the tethered drug moieties are fixed at the device's surface and can neither migrate into nor build up to a high drug concentration in the surrounding tissue despite the fact that a high drug concentration during the critical postimplantation period is required for better improvement of the postimplantation reaction.^{16,19} Moreover, this approach requires different drugs to be individually customized onto the surface of the devices. Installing a drug-release character to any PDMS materials has also been carried out by directly dispersing drug molecules into a polymeric matrix.^{20,21} Nevertheless, this direct mixing method is only popular in pharmaceutical preparations and devices, such as a silicone elastomer vaginal gel with antiviral activity,²² intravaginal drug-delivery rings,^{23–25} and transdermal drug-delivery patches,²⁶ in which the mechanical properties and long-term stability of the devices are not critical. To conserve the mechanical and viscoelastic properties of PDMS medical devices, only limited amounts of drugs could be mixed into the polymeric matrix; thus, the release of sufficient amounts of drugs could not be attained through this strategy.¹⁴

Therefore, a platform that allows the deposition of diverse drugs onto the device's surface in an adequate quantity with reliable attachment and a sustained-release character is needed. Here, a novel platform for covalent linking of nanodepots filled with a high amount of drug molecules to the surface of PDMS was developed for the first time. The platform offers the secure attachment and ability to release drug molecules into the surrounding tissue, as well as an increased hydrophilicity of the PDMS surface, without altering the key physical characteristics of the bulk PDMS material.

Endotracheal tubes for assisted ventilation are a high-risk medical device in terms of infection and inflammation because of their location and function.¹ As a result, the tracheal tube was chosen as a representative PDMS medical device with budesonide, a hydrophobic drug with antiinflammatory activity, as a representative drug to be deposited onto the tube surface. Here surface functionalization of the PDMS tracheostomy tube, to make it both hydrophilic and able to slowly release budesonide, was developed by loading budesonide into ethylcellulose (EC) nanoparticles and then covalently linking the budesonide–EC nanoparticles onto the functionalized PDMS tube. The process was confirmed by scanning electron microscopy (SEM) and confocal fluorescent microscopy (CLFM). The budesonide loading level was evaluated along with its subsequent *in vitro* release over a 4-week period. The physical property of the (budesonide-loaded particle)-grafted PDMS tubes was compared to that of the untreated PDMS tubes in terms of their hardness (Shore-A) and surface hydrophilic nature. The obtained (budesonide-loaded particle)-grafted PDMS tubes were tested for their *in vitro* and *in vivo* antiinflammatory activity in cell culture and after implantation into rats, respectively.

EXPERIMENTAL SECTION

The PDMS tubes with a 10.0 mm outer diameter and 8.00 mm inner diameter were obtained from Koken (Tokyo, Japan), while EC [48% (w/w) ethoxy content and a viscosity of 300 cP] and 1-hydroxybenzotriazole (HOBt) were from Sigma-Aldrich (Steinheim,

Germany). Budesonide ($M_w = 430.5$, analytical grade) was purchased from Fluka (Seelze, Germany). Succinic anhydride (analytical grade), (3-aminopropyl)triethoxysilane (γ -APS), and 1-ethyl-3-[3-(dimethylamino)propyl]carbodiimide–HCl (EDCI) were purchased from Acros Organics (Geel, Belgium). Rhodamine B sulfonyl chloride was purchased from Invitrogen (Grand Island, NY).

UV–vis spectroscopy was obtained from a UV-2550 spectrometer (Shimadzu, Japan). SEM and transmission electron microscopy (TEM) were performed using JEM-6400 (JEOL, Japan) and JEM-2100 (JEOL, Japan) instruments, respectively. Dynamic light scattering (DLS) was performed on a Zetasizer nanoseries instrument (Zs, Malvern Instruments, USA). The water contact angle was obtained using a Ramé-Hart model 200 standard contact angle goniometer (Succasunna, NJ). Fluorescent images were obtained by CLFM using a Nikon Digital Eclipse C1si confocal microscope system (Tokyo, Japan) equipped with Plan Apochromat VC 100X, a Melles Griot diode laser and a 85 YCA-series laser at 561 nm, a Nikon TE2000-U microscope, a 32-channel PMT spectral detector, and Nikon-EZ-C1 Gold Version 3.80 software. The hardness (Shore-A) of the materials was measured using a Durometer model 408 type A (Shore-A; PTC Instruments, Los Angeles, CA). ¹H NMR spectra were obtained in deuterated chloroform ($CDCl_3$) with tetramethylsilane as an internal reference using an ACF 200 spectrometer, which operated at 400 MHz for ¹H nuclei (Varian Co., Palo Alto, CA).

Encapsulation of Budesonide into EC Nanoparticles. The encapsulation of budesonide into EC nanoparticles was performed at a 1:1 (w/w) ratio of budesonide–EC by solvent displacement.²⁷ Budesonide (500 mg) and EC (500 mg) were dissolved in ethanol (EtOH) to give EC and budesonide each a 5 mg/mL final concentration. The mixture (50 mL) was dialyzed against distilled water (5×1000 mL, using a CelluSep T4 membrane, M_w cutoff (M_wCO) of 12–14 kDa; Membrane Filtration Products, Seguin, TX). An aqueous suspension of budesonide-loaded EC particles obtained inside the dialysis bag was collected. The morphology and size of the dry budesonide-loaded EC particles were evaluated by SEM and TEM, while the hydrated size was determined by DLS. The amounts of budesonide in the particles and those in the dialysate water were determined using UV–vis absorption spectroscopy at 246 nm, with the aid of a calibration curve constructed with 5, 10, 15, 20, 25, 30, and 35 ppm standard budesonide solutions. The encapsulation efficiency (EE) and loading capacity were calculated from eqs 1 and 2, respectively:

$$EE (\%) = (A/B) \times 100 \quad (1)$$

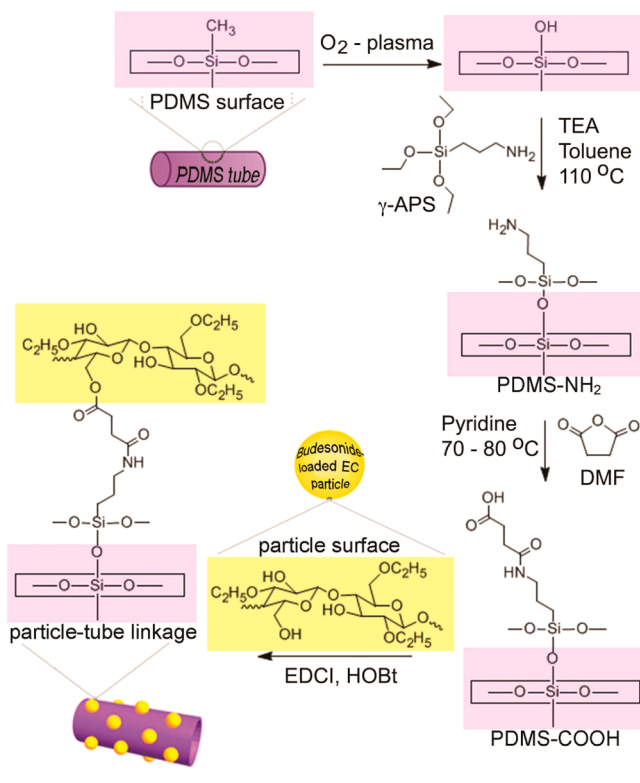
$$\text{loading capacity} (\%) = (A/C) \times 100 \quad (2)$$

where *A* is the weight of encapsulated budesonide, *B* is the weight of budesonide originally used, and *C* is the weight of the obtained budesonide-loaded particles.

The obtained budesonide-loaded EC nanoparticle suspension was then freeze-dried.

Fluorescence-Labeled Particles. The fluorophore Rhodamine B was covalently linked to the EC particles by adding 0.5 mL of a 1% (w/v) Rhodamine B into 200 mL of an aqueous EC nanoparticle suspension (2.5 mg/mL) in the presence of a catalytic amount (2 drops) of pyridine under a light-proof and nitrogen (N_2) atmosphere (Scheme S1 in the Supporting Information, SI). The mixture was stirred at room temperature overnight. The Rhodamine B-labeled EC polymer was then purified from free Rhodamine B by dialysis under light-proof conditions.

Surface Treatment of the PDMS Tubes (Scheme 1). The PDMS tubes were first subjected to oxygen plasma treatment (STERRAD100S, ASP, Irvine, CA) using a standard disinfection condition which was at 55–60 °C with radio waves and hydrogen peroxide (H_2O_2) for 10 cycles. The cycle was composed of a sequential vacuum (397 mTorr, 20 min 16 s), injection (6.34 Torr, 6 min 2 s), diffusion (15 Torr, 2 min), plasma (552 mTorr, 7 min 23 s), injection (7.67 Torr, 6 min 2 s), diffusion (15 Torr, 2 min), plasma (630 mTorr, 7 min 11 s), and vent stages. The hydrophilic/

Scheme 1. Grafting of Budesonide-Loaded EC Particles onto the Surface of a PDMS Tube

hydrophobic nature of the obtained tubes was then evaluated by measuring the water contact angle.

Condensation between the silanol groups on the surface of the plasma-treated PDMS tubes with γ -APS was then performed using a method modified from that previously described.²⁸ Briefly, the plasma-treated PDMS tubes (130 cm² total surface area) were cut into 1 cm pieces and then refluxed in 50 mL of 2% (v/v) γ -APS in toluene with 2–3 drops of triethanolamine for 3 h under a N₂ atmosphere. The tubes were then removed from the solution, sequentially rinsed with water (1000 mL), hexane (40 mL), and EtOH (40 mL), and annealed at room temperature for 24 h. The washed tubes were dried in a desiccator for 24 h to obtain the amino-functionalized PDMS (PDMS-NH₂) tubes. The product was characterized for the presence of surface primary amino groups by the Kaiser test.²⁹

The PDMS-NH₂ tubes (130 cm² total surface area) were then stirred in a solution of succinic anhydride (1 g) in 50 mL of dimethylformamide with 2–3 drops of pyridine at 70 °C overnight under a N₂ atmosphere. Free succinic anhydride and succinic acid were eliminated by washing the obtained tubes with excess water. The obtained carboxyl PDMS (PDMS-COOH) tubes were then subjected to the Kaiser test.

For the Kaiser test, the tubes were soaked in a 0.1% (w/v) ninhydrin solution in EtOH and then heated at 50–60 °C for 1 min to activate the reaction. The color change was visually observed.

Grafting the Surface of the PDMS-COOH Tube with Budesonide-Loaded EC Particles (Scheme 1). To have the surface of PDMS-COOH grafted with the budesonide-loaded EC particles, a 50 mL aqueous suspension of budesonide-loaded EC nanoparticles (containing 125 mg of budesonide and 250 mg of EC) was put into a round-bottomed flask and HOBt (0.88 g, 0.65 mol) in EtOH (5 mL) was added. The PDMS-COOH tubes (4.40 cm² surface area per tube, 30 tubes) and EDCI (1.25 g, 0.65 mol) were added into the flask, and the mixture was stirred at 0 °C under a N₂ atmosphere overnight. The grafted tubes (denoted as budesonide-loaded PDMS tubes) were then rinsed with excess water repeatedly, followed by 20 mL of EtOH, and then dried before being subjected to SEM and hardness (Shore-A) analyses.

PDMS-COOH tubes were also grafted with fluorescent EC particles using a similar procedure, and the obtained fluorescent-particle-grafted tube was subjected to CLFM analysis (excitation at 561 nm and detection by scanning from 565 to 700 nm).

The amount of budesonide deposited onto the tubes was quantified by subjecting the tubes to EtOH extraction. The ethanolic extract was centrifugally filtered through a membrane (M_wCO of 10 kDa) to filter out EC, and the supernatant was subjected to high-performance liquid chromatography (HPLC) analysis with the aid of a calibration curve. The extracted budesonide was also dried, redissolved in CDCl₃, and subjected to ¹H NMR analysis.

In Vitro Budesonide Release. The budesonide-loaded PDMS tubes (seven tubes, 4.40 cm² surface area per tube) were submerged in 5.0 mL of a release medium [0.075 mM phosphate buffer saline solution (pH 5.8), 5% (v/v) Tween 20, and 20% EtOH] at 37 °C. Aliquots of the release medium (500 μ L each) were transferred into micro centrifuge tubes at the indicated times (0, 1, 2, 5, 8, 9, 10, 12, and 14 days). The volume of the release medium was kept constant by adding fresh release medium (500 μ L each) after each sampling. The withdrawn aliquot was gently preconcentrated under a N₂ gas flow to a final volume of ~200–300 μ L, whereupon 200 μ L of ethyl acetate was added, the mixture was vortexed and allowed to phase separate, and the ethyl acetate layer was collected. The budesonide concentration in the ethyl acetate layer was then quantified using HPLC analysis with the aid of a calibration curve constructed from budesonide standard solutions freshly prepared in ethyl acetate.

HPLC Analysis. HPLC analysis was performed using a Waters 1525 binary high-performance liquid chromatograph (pump) and a 100 mm \times 4.6 mm column packed with Hypersil C18 (Thermo Fisher Inc., Waltham, MA) and connected to a Waters 2489 UV–vis detector (Milford, MA) operating at 240 nm. The sample injection volume was 10 μ L, the mobile phase was a 2:30:68 (v/v/v) EtOH–acetonitrile–25 mM phosphate buffer (pH 3) mixture, and the flow rate was 1.5 mL/min.

In Vitro Antiinflammatory Activity in Cell Culture. The unmodified PDMS (control) and the budesonide-loaded PDMS tubes were subjected to an in vitro antiinflammatory test in tissue culture using the RAW264.7 (ATCC TIB-71) mouse macrophage-like cell line. The tubes were cut into 0.5 \times 0.6 cm pieces (2 mm thick). For the budesonide-loaded PDMS pieces, both sides were grafted with budesonide-loaded EC particles and contained 15 μ g of budesonide/piece. The tubes were autoclaved prior to use. These were evaluated along with a culture control (no test sample added) and free budesonide.

Cells were maintained in a complete medium [CM; Dulbecco's modified Eagle medium supplemented with 10% (v/v) fetal bovine serum, 1% (w/v) sodium pyruvate, 1% (w/v) N-2-hydroxyethylpiperazine-N'-2-ethanesulfonic acid (Hyclone), 100 U/mL penicillin, and 0.25 mg/mL streptomycin] and were incubated at 37 °C in a humidified 5% (v/v) CO₂ incubator. Cells were plated overnight in a 24-well plate (5 \times 10⁴ cells/well) in CM. The medium was changed to fresh CM before the addition of the respective treatment (nothing, budesonide (15 μ g), and unmodified or budesonide-loaded PDMS pieces) for 48 h. The medium was then replaced with fresh CM, and the RAW264.7 cells were stimulated with 100 ng/mL lipopolysaccharide (LPS from Salmonella) and 10 ng/mL interferon- γ (IFN γ) for 24 h. The culture supernatant was then harvested, and the concentration of nitric oxide (NO) was measured using the Griess reaction as described previously.³⁰

In Vivo Antiinflammatory Activity in Rat Implants. The procedures were approved by both the Ethics Committee and the Institutional Animal Care and Use Committee of Chulalongkorn University. The unmodified and budesonide-loaded PDMS pieces were subjected to an in vivo antiinflammatory test by subcutaneous implantation in rats, according to the biological evaluation of medical devices of international standard ISO10993-6:2007 (E). The unmodified and budesonide-loaded PDMS pieces were prepared as described above, except that each piece was 1.0 \times 0.6 cm in size and so contained 30 μ g of budesonide/piece (for the budesonide-loaded PDMS pieces). The autoclaved pieces were used in the experiment.

In total, nine male Wistar rats, 12 weeks old (National Laboratory Animal Center, Nakorn Pathom, Thailand), were surgically implanted with the PDMS pieces on one side of the dorsal subcutaneous tissue of the back and the budesonide-loaded PDMS pieces on the other side (sides chosen at random) under ketamine hydrochloride and xylazine hydrochloride general anesthesia. Each set of three randomized animals was sacrificed, and the skin samples were removed after 7, 14, and 28 days postsurgery, respectively. The skin samples were fixed in 10% (w/v) buffered formalin and histopathologically examined by hematoxylin and eosin (H&E) staining. Semiquantitative evaluation of the degree of inflammation was performed by histopathological grading according to the ISO10993-6:2007(E) Annex E.

RESULTS AND DISCUSSION

Budesonide-Loaded Carriers. Budesonide was successfully encapsulated into the EC nanoparticles by solvent displacement. The aqueous suspension of the budesonide-loaded EC nanoparticles formed inside the dialysis bag appeared as a milky white suspension (Figure 1). The SEM

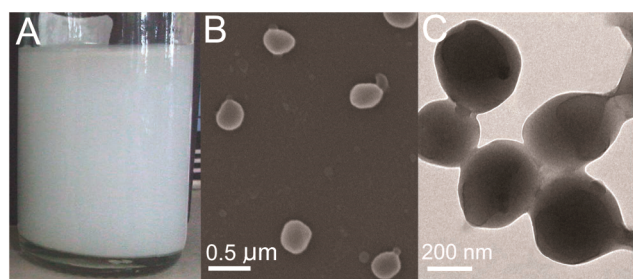


Figure 1. Budesonide-loaded EC particles: (A) aqueous suspension of budesonide-loaded EC nanoparticles (concentrations of budesonide and EC of 1.25 and 2.50 mg/mL, respectively) and representative (B) SEM and (C) TEM images of the budesonide-loaded EC nanoparticles.

and TEM images of the product (Figure 1) revealed a spherical morphology with an anhydrous particle size of 342.10 ± 85.04 nm, while DLS gave a slightly larger hydrodynamic diameter of 356 nm with a polydispersity index of 0.256 (midrange polydispersity). The mean ζ potential of the budesonide-loaded EC nanoparticles in water at pH 6.5 was -57.40 ± 1.27 mV, agreeing well with the observed stable particle suspension over 3 months.

Centrifugal filtration of the particle suspension allowed separation of the unencapsulated budesonide (filtrate) from the budesonide-loaded EC particles (residue), and the filtrate was quantified for budesonide concentration by UV absorption spectrophotometry with the aid of a calibration curve (see Figure S1 in the SI for the calibration curve). The result indicated that the obtained budesonide-loaded EC nanoparticles had a high loading capacity [$33.26 \pm 0.23\%$ (w/w)] and the encapsulation process gave a moderate EE ($49.83 \pm 0.11\%$). It should be noted here that the encapsulation process was performed at a 1:1 (w/w) ratio of budesonide–EC. The optimized condition used here gave particles with no budesonide crystal/precipitate.

During dialysis of the ethanolic solution containing EC and budesonide, when EtOH was slowly displaced with water, it was likely that the EC chains self-assembled themselves in such a way that the hydrophilic hydroxyl groups were in maximum contact with the water medium while the hydrophobic ethoxyl groups were at the inside of the forming particles away from the water medium, resulting in budesonide-loaded EC particulates

with a hydrophilic outer surface and a hydrophobic interior.²⁷ During particle formation, the hydrophobic nature of budesonide probably drove the molecules to the hydrophobic core of the forming spheres, leading to encapsulation of budesonide inside the forming EC particles.

The fact that the particles were loaded with the hydrophobic budesonide molecules at 33% loading content agreed well with this molecular assembling speculation. In addition, the observation that a fast addition of water into an EC solution (in EtOH) produced water-undispersible precipitates while slow displacement of EtOH in the EC solution with water through dialysis resulted in water-dispersible nanospheres also conformed well with the proposed self-assembling speculation.

Surface Functionalization of PDMS Tubes (Scheme 1). To make PDMS tubes that were able to slowly release budesonide while still maintaining their bulk properties, only the surface of the tubes was covalently linked to the budesonide-loaded EC nanoparticles. The process was comprised of the four steps: (i) activation of the PDMS surface with oxygen plasma to introduce silanol moieties onto the surface (plasma-treated PDMS); (ii) silanization of the plasma-treated PDMS surface with γ -APS to introduce amino groups onto the tubes' surface (PDMS-NH₂); (iii) coupling of the amino groups with succinic anhydride to introduce carboxylic groups onto the tubes' surface (PDMS-COOH); (iv) linking of the hydroxyl groups on the outer surface of the budesonide-loaded EC particles to the carboxylic groups on the surface of the PDMS-COOH tubes through ester bonds (budesonide-loaded PDMS), as shown in Scheme 1.

Because the surface of the PDMS tubes is quite inert, activation of the surface by oxygen plasma was first performed to introduce silanol (Si–OH) moieties onto the surface via a free-radical oxidation mechanism. This treatment rendered the PDMS surface hydrophilic, which was verified by the change in the water contact angle from $107.28 \pm 1.9^\circ$ for the untreated PDMS surface to $71.6 \pm 6.5^\circ$ for the plasma-treated surface. Note that the water contact angle was measured soon after the plasma treatment was completed because, theoretically, the resulting silanol groups on the plasma-treated PDMS could undergo cross-linking into stable siloxane linkages. The plasma-treated PDMS tubes were then quickly silanized by reaction with γ -APS to introduce amino groups onto their surface via a base-catalyzed hydrolysis–condensation between the silanol groups and γ -APS to yield the covalent siloxane network with aminopropyl moieties on the outer surface of the tubes (PDMS-NH₂).³¹

Attempts to verify the chemical change at the surface of the plasma-treated tubes with attenuated total reflectance Fourier transform infrared spectroscopy (ATR-FTIR) analysis failed because the IR spectrum of the freshly prepared plasma-treated PDMS and that of the untreated PDMS tubes were the same. This was likely because not only was functionalization attained at the top surface of the material but also ATR-FTIR detection acquired information on the sample at a depth of more than 60–70 nm from the surface. Attempts to scratch the functionalized surface off and powder it so as to then make a KBr compression disk also failed because PDMS was too elastomeric to scratch. Nevertheless, in addition to the water contact-angle information, the successful coupling with γ -APS confirmed the presence of the silanol groups on the surface of the plasma-treated PDMS tubes.

The presence of the amino functionality on the surface of the thoroughly washed and annealed tubes was confirmed by

coloration with the Kaiser reagent,²⁹ in which a deep-violet-blue color on the tube surface was clearly observed (Figure S2 in the SI). The obtained amino-functionalized tubes were stable and could be kept in a desiccator until needed.

Here, the plan was to covalently link the budesonide-loaded EC particles to the surface of the PDMS tubes so the budesonide-loaded EC particles could act as drug depots at the tubes' surface. Many of the hydroxyl groups on the EC chains should be exposed at the outer surface of the budesonide-loaded EC particles and so could be used for covalent linking to the functionalized PDMS. Thus, carboxylic groups were introduced onto the surface of the tubes to serve as a reactive functionality for linking with the hydroxyl groups on the EC particles via ester linkage. Accordingly, the PDMS-NH₂ tubes were reacted with succinic anhydride to produce the PDMS-COOH tubes (Scheme 1). Successful coupling was verified through the negative Kaiser test (Figure S3 in the SI).

Finally, the PDMS-COOH tubes were grafted with the budesonide-loaded EC particles through the formation of ester linkages between the surface hydroxyl and carboxyl groups of the particles and the tubes, respectively (Scheme 1). The SEM images of the obtained budesonide-loaded PDMS tubes clearly indicated the presence of particles on the surface of the tube (Figure 2A), and their size resembled that of the budesonide-loaded EC particles (Figure 1). To more clearly characterize the distribution of the particles on the tube's surface, the EC particles were first covalently labeled with Rhodamine B, a fluorescent chromophore, and then the PDMS-COOH tubes were grafted with the fluorescent EC particles using a process similar to that above. The obtained (fluorescent EC particle)-grafted PDMS tubes showed an obvious fluorescence signal on their surfaces with an islandlike distribution of particles on the tube's surface (Figure 2B). Factors affecting the distribution of particles on the surface probably included the distribution of -COOH functionalities on the surface (starting from the plasma treatment step) and also agitation during the reaction between PDMS-COOH and the particles. Nevertheless, an improved hydrophilic nature of the grafted tubes was observed; i.e., the budesonide-loaded tubes showed a better wetting with a water contact angle of $48.6 \pm 8.5^\circ$ compared to $107.28 \pm 1.9^\circ$ for the unmodified PDMS tubes. Overall, the data support that the tube's surface was grafted with the particles. The size and thickness of the tubes did not change upon functionalization, but the surface of the budesonide-loaded PDMS tubes appeared more opaque compared to that of the unmodified tubes (Figure 2C,D).

Quantification of the budesonide level on budesonide-loaded PDMS tubes using EtOH extraction followed by quantification with HPLC, revealed that, under the grafting condition used, the average budesonide coverage on the tube's surface was 0.0254 ± 0.022 mg/cm². Here HPLC was used to quantify budesonide in the extract, instead of the previously used direct UV absorption analysis, in order to make sure that UV absorption detected at 240 nm was only from budesonide and not from other components that might be extracted from the tubes. Note here that, under the HPLC condition used, the retention time of budesonide was approximately 11 min and the linear calibration curve was obtained for the 10–50 ppm budesonide standards (Figure S4 in the SI). Because the extracted budesonide retained its chemical structure (verified by ¹H NMR), it was concluded that no harm was done to the drug molecules during the grafting process and so the PDMS surface could be noncovalently loaded with budesonide by

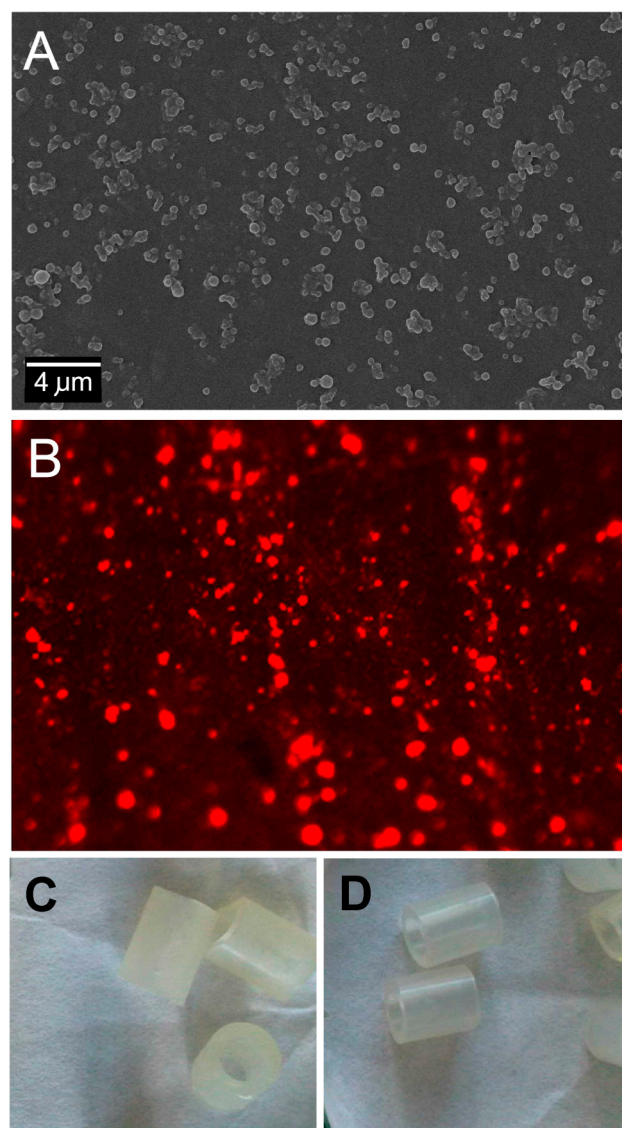


Figure 2. Images of PDMS tubes. SEM (A) and fluorescence (B) images of the surface of the (budesonide-loaded EC particle)-grafted PDMS tube. Photographs of the (budesonide-loaded EC particle)-grafted PDMS tubes (C) and original PDMS tubes (D).

covalent linking of the budesonide-loaded EC particles to its surface. This allows the accumulation of a high drug content on the limited surface area. More importantly, the accumulated drug molecules were not destroyed by the reaction that linked the particles to the PDMS surface. These linked particles should act as drug depots on the PDMS surface to release active drug molecules in situ during use, and this was evaluated next.

To make sure that the grafting of the tube's surface with budesonide-loaded EC nanoparticles did not significantly alter any important physical properties of the tube, the hardness (Shore-A) of the tube as a representative and key character was measured using a durometer. Numerically similar values of 26.3 ± 2.1 and 28.1 ± 0.6 were obtained for the unmodified and the budesonide-loaded PDMS tubes, respectively, and these were not significantly different ($P \leq 0.05$; Mann–Whitney U test). Note that a direct comparison of the hardness between the budesonide-loaded and unmodified PDMS tubes was possible because they had the same thickness (2 mm). Thus, the surface

treatment did not significantly change the hardness, a key physical property, of the PDMS tubes.

Budesonide Release. The *in vitro* release of budesonide from the budesonide-loaded PDMS tubes was evaluated in the release buffer of pH 5.8. An initial fast release followed by a slower release at a later time was observed (Figure 3); thus, the

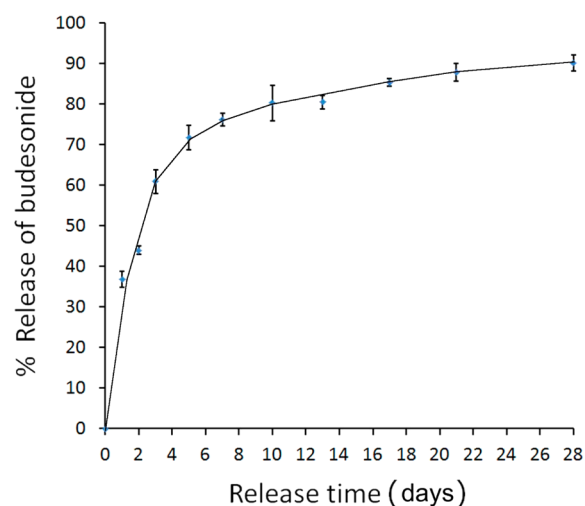


Figure 3. Release of budesonide from the budesonide-loaded PDMS tubes when immersed in a release buffer at 37 °C. Data are shown as mean \pm 1 standard deviation and are derived from three independent repeats.

release mechanism was a passive diffusion driven by the concentration gradient between the inside and outside of the particles, in which the EC matrix acted as a diffusion barrier. The fast release during the first week was a result of the high drug concentration gradient between the inside and outside of the grafted particles. The fastest release during day 1 was expected because the concentration difference was maximal. The fast release during the first few days fulfills the requirement of providing a high drug concentration during the critical first few days postimplantation. Thereafter, the release rate decreased as the concentration gradient decreased and became essentially constant after 1 week, which is probably controlled by the rate of diffusion through the EC matrix of the budesonide molecules that was located deep inside the grafted particles. It should be noted here that EC is stable at alkaline pH, down to a pH value of approximately 4; therefore, the sustained release character of the encapsulated drug from the tube's surface could be expected in applications at pH above 4. Nevertheless, an actual release character will be affected greatly by the environment around the tube. Although the release of budesonide from the surface of the budesonide-loaded PDMS tubes shown here did not exactly represent the true *in situ* (*in vivo*) release at the contact tissue in a real application, the results still confirmed the sustained drug-release characteristic of the budesonide-loaded PDMS tubes. An ability to release budesonide from the budesonide-loaded tubes was also tested in two more circumstances, in a tissue culture medium and in contact with the rat's tissue under real implantation, and the results and discussions are presented next.

In Vitro Antiinflammatory Activity in Cell Culture.

Treatment of the macrophage-like cell line RAW264.7 *in vitro* with the budesonide-loaded PDMS tubes in the presence of LPS and IFN- γ resulted in a significantly lower NO production

level than that for treatment with the unmodified PDMS (Figure 4). This implied that budesonide inside the grafted particles on the tubes could be released into the culture medium and performed *in vitro* antiinflammatory action to the cells.

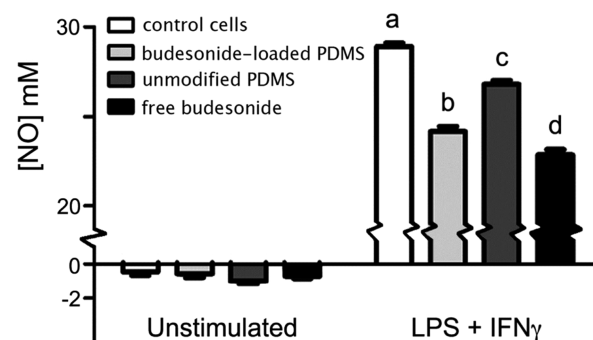


Figure 4. *In vitro* antiinflammatory activity (shown as a decreased NO production level) of the budesonide-loaded PDMS when tested on the LPS- and IFN- γ -costimulated RAW264.7 macrophage cell line, in comparison with free budesonide (at the same amount of budesonide as that in the budesonide-loaded PDMS sample) and the unmodified PDMS. Data are shown as the mean \pm 1 standard deviation and are derived from three independent repeats. Different letters on the data bars indicate the statistical significant difference between the sample, as determined by one way ANOVA Duncan at $P < 0.05$.

3.5. In Vivo Antiinflammatory Activity in Implanted

Rats. Evaluation of the tissue surrounding the subcutaneous implanted budesonide-loaded and unmodified PDMS (control) tubes in nine male Wistar rats was performed visually and by histopathological examination under a light microscope. Visual observation of the implant area at day 7 postimplantation revealed no large differences in the tissue reactions in the area surrounding either the unmodified or budesonide-loaded PDMS tube implants; the surgical reactions had masked any development of specific inflammation and tissue reactions. At 14, 21, and 28 days postimplantation, however, the area around the budesonide-loaded PDMS implants showed significantly less inflammation.

Subcutaneous implantation of a medical device usually creates a wound that triggers the host inflammatory response and infiltration of phagocytic cells, such as polymorphonuclear cells, lymphocytes, macrophages, and giant and mast cells. Here, the amounts of these cells were observed by histopathological examination via H&E staining. A significantly lower inflammatory cell infiltration level and less tissue responses in the tissues surrounding the budesonide-loaded PDMS implants were observed during the 28-day post-implantation period compared to those surrounding the unmodified PDMS ones (Table 1). At the 7th and 14th day postimplantation, all of the rats showed a significantly lower number of the five types of inflammatory cells in the area surrounding the budesonide-loaded PDMS implant, compared to the control area in the same rat in each case. On the 28th day postimplantation, polymorphonuclear cells could not be observed in the surrounding area of either the budesonide-loaded or control PDMS implants, and fewer macrophages and lymphocytes were observed around the area implanted with the budesonide-loaded PDMS tubes compared to that around the control PDMS implants. In addition, no giant or mast cells were observed around the budesonide-loaded PDMS implants

Table 1. Histopathological Findings of the Cellular and Tissue Responses in the Tissues around the Implanted Materials^a

| day | PDMS type | cell type ^b | | | | | tissue response ^c | | | |
|-----|-------------------|-------------------------|-------------|-------------|-------------|------------|------------------------------|------------|----------|--------------------|
| | | polymorphonuclear cells | lymphocytes | macrophages | giant cells | mast cells | fibrin clot | hemorrhage | fibrosis | neovascularization |
| 7 | unmodified | 2 | 3 | 3 | 1 | 1 | 2 | 1 | 1 | 1 |
| | budesonide-loaded | 1 | 1 | 2 | 0 | 0 | 1 | 0 | 1 | 1 |
| 14 | unmodified | 1 | 2 | 3 | 1 | 2 | 0 | 0 | 2 | 3 |
| | budesonide-loaded | 0 | 1 | 1 | 0 | 0 | 0 | 0 | 1 | 1 |
| 28 | unmodified | 0 | 2 | 3 | 1 | 1 | 0 | 0 | 3 | 2 |
| | budesonide-loaded | 0 | 1 | 1 | 0 | 0 | 0 | 0 | 2 | 1 |

^aData shown are the average from the nine rats (three rats per group for each time point). ^bCell types: phf = per high power field (400×); 0 = none, 1 = 1–5 cells/phf, 2 = 5–10 cells/phf, 3 = heavy infiltrate, and 4 = packed; graded from more than nine slides obtained from each surgical implant wound (a total of more than 27 slides for each sample at each time point). ^cTissue responses: 0 = none, 1 = minimal, 2 = mild, 3 = moderate, and 4 = severe; graded from three rats at each time point.

in contrast to the control PDMS implants. The tissue responses examined, which included fibrin clots, hemorrhage, fibrosis, and neovascularization, were all significantly less pronounced in the area surrounding the budesonide-loaded PDMS implants than the control PDMS implants in all nine rats during the 28-day postimplantation period (Table 1). Representative H&E-stained tissue samples at the 28th day postimplantation are shown in Figure 5, with inflammatory cells clearly identifiable by their dark-purple nuclei. The tissue at the implant interface of the control (unmodified PDMS) showed infiltration of a

large number of inflammatory cells, whereas that adjacent to the budesonide-loaded PDMS implants exhibited a markedly lower inflammatory response, as evidenced by fewer cells and a thinner fibrous tissue level.

The lower inflammatory and tissue responses observed in the budesonide-loaded PDMS implants compared to the unmodified PDMS ones were likely to have resulted from the continuous release of budesonide, an antiinflammatory drug, from the surface of the budesonide-loaded PDMS implants into the surrounding tissues. In addition, the more hydrophilic surface of the budesonide-loaded PDMS implant should reduce the irritation, abrasion, and dead space between the implant and the tissue^{7,8} and so contributed to the reduction in the inflammation and tissue responses. Four key points should be noted for this particle-grafted PDMS platform (illustrated here as budesonide-loaded PDMS). First, the covalent linkage of the carrier particles (EC in this case) to the modified PDMS surface provides a secure attachment of the drug carrier at the device's surface, and so detachment during storage or use is unlikely. This is different from previous reports that have relied on the noncovalent binding.^{14,32} Second, this platform gave devices with a high drug surface coverage without any deep alteration to the bulk (PDMS) material. Thus, the hardness, a key physical property of the bulk platform, remained unchanged. This is different from the direct mixing of drugs into the polymer matrix in which intense alterations of mechanical and viscoelastic properties and material homogeneity of the devices could be observed even at low drug loading.¹⁴ Third, the drug molecules were not covalently linked to the surface but were intended to be released and diffuse away from the immediate implant surface to be able to perform their bioactivity in the surrounding tissue (in this case, the antiinflammatory activity of budesonide as the payload drug). In other words, this new platform provides a secure grafting, yet the drug molecules are still releasable. This is different from the direct grafting of the drug molecules onto the surface where they remain tethered without any active release^{16–18} and so exert no biological activity away from the implant surface and would also be poor delivery agents for drugs requiring cellular internalization for full bioactivity. The platform presented here provides a secure deposit of drugs for subsequent active release from the PDMS surface. The flexibility of the platform, in terms of an easy change of the payload drug (or even drugs), should allow a fast exploration for making other PDMS medical devices with the active release of various drugs. Here, we used nanocarriers made from EC as a model payload carrier, but carriers made of other materials should also be useable.

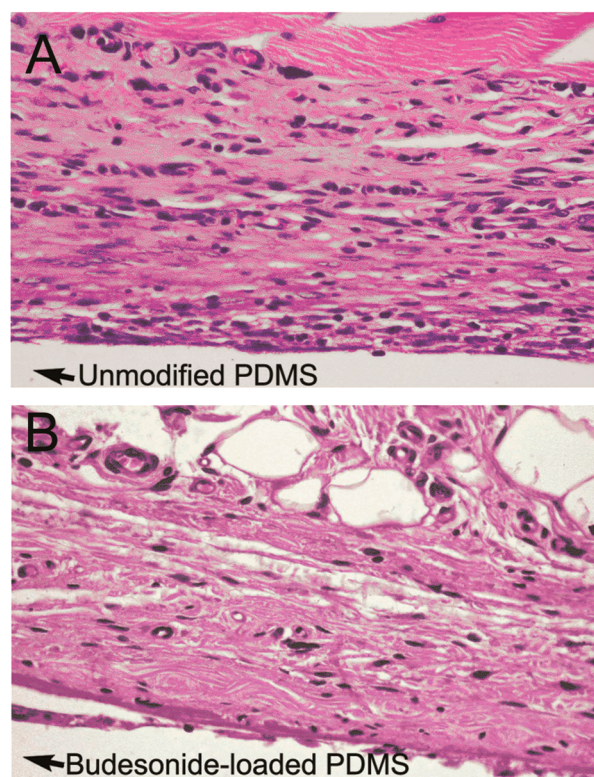


Figure 5. Histopathology of the H&E-stained subcutaneous tissue after 4 weeks postimplantation. Optical micrographs (400× magnification) showing the fibrous tissue surrounding the (A) unmodified PDMS implant and (B) the budesonide-loaded PDMS implant. Nuclei of inflammatory cells are stained dark purple, while the collagen appears pink (H&E stain). The implant was located at the bottom white region (denoted with an arrow) of each image. Each image shown here is a representative of more than nine images obtained from each of the three rats (total of more than 27 slides).

Nevertheless, nanocarriers made from EC are easy to fabricate and have a demonstrated ability to encapsulate many hydrophobic drugs with a high loading capacity.^{27,33,34} Fourth and last, the use of nanoparticles with a hydrophilic outer surface also rendered the grafted PDMS surface hydrophilic, and this is important for better tissue contact. This will also help to reduce the problem of the dead space between the implant and the tissue that is encountered with the unmodified hydrophobic PDMS surface and so minimize the bacterial colonization and abrasion. In fact, this was observed in the implantations in rats in this study, where lower tissue responses and less inflammation were observed.

CONCLUSION

Here silicone tracheostomy tubes with a sustained release of budesonide were prepared by covalently grafting the surface of the PDMS tubes with the budesonide-loaded EC nanoparticles. First, silanol groups were introduced onto the surface of the PDMS tubes by oxygen plasma treatment, and then the plasma-treated PDMS tubes were subjected to a condensation reaction with γ -APS to yield PDMS tubes with amino groups on their surface (PDMS-NH₂). The coupling of PDMS-NH₂ with succinic anhydride then yielded tubes with carboxylic moieties on the surface, and these PDMS-COOH tubes were then esterified with the hydroxyl groups on the surface of the budesonide-loaded EC particles to yield the budesonide-loaded PDMS tubes. A high budesonide loading level of the attached spheres of 33.26% (w/w) was obtained, resulting in a high budesonide coverage of 0.025 mg/cm² at the tube's surface. Importantly, because the functionalization was restricted to only the surface of the tube, the hardness of the bulk PDMS material was not significantly changed. Sustained in vitro release of the payload budesonide from the budesonide-loaded PDMS tubes was observed for 4 weeks, and so the grafted budesonide-loaded EC particles acted as nanodrug depots on the device surface. The budesonide-loaded tubes could be kept at room temperature and autoclaved prior to use. Although grafting of the PDMS surface with the drug-loaded particles is shown here for a tracheostomy tube with budesonide as the demonstrated drug and EC particle as the depot, the platform could theoretically be applied to different PDMS medical devices and other payload drugs and not only to indwelling devices but also to permanent implants requiring a controlled release of drug during the critical initial postimplantation period and so should be a significant improvement in the success of implantations.

ASSOCIATED CONTENT

Supporting Information

Labeling EC particles with Rhodamine B, colorimetric Kaiser test for amine groups on the surface of unmodified PDMS and PDMS-NH₂ tubes and of the PDMS-NH₂ tubes before and after treatment with succinic anhydride. This material is available free of charge via the Internet at <http://pubs.acs.org>.

AUTHOR INFORMATION

Corresponding Author

*E-mail: psupason@chula.ac.th.

Funding

This work was financially supported by the Ratchadapiseksompot Endowment Fund of Chulalongkorn University

(RESS60530097-Adv Mat) and Nanotec-CU Center of Excellence on Food and Agriculture.

Notes

The authors declare no competing financial interest.

ABBREVIATIONS

PDMS, poly(dimethylsiloxane)
PDMS-NH₂, amino-functionalized poly(dimethylsiloxane)
PDMS-COOH, carboxyl-functionalized poly(dimethylsiloxane)
budesonide-loaded PDMS, poly(dimethylsiloxane) grafted with budesonide-loaded particles
 γ -APS, (3-aminopropyl)triethoxysilane

REFERENCES

- (1) Brown, M. T.; Montgomery, W. W. Microbiology of Tracheal Granulation Tissue Associated with Silicone Airway Prosthesis. *Ann. Otol., Rhinol., Laryngol.* **1996**, *105*, 624–627.
- (2) Mesleman, D.; Yaremchuk, K.; Rontal, M. The Presence of Biofilms on Adult Tracheotomy Tubes. *Laryngoscope* **2009**, *119* (Supplement 1), 122.
- (3) Kourtzelis, I.; Rafail, S.; DeAngelis, R. A.; Foukas, P. G.; Ricklin, D.; Lambris, J. D. Inhibition of Biomaterial-Induced Complement Activation Attenuates the Inflammatory Host Response to Implantation. *FASEB J.* **2013**, *27*, 2768–2776.
- (4) Xu, D.; Yang, W.; Hu, Y.; Luo, Z.; Li, J.; Hou, Y.; Liu, Y.; Cai, K. Surface Functionalization of Titanium Substrates with Cecropin B to Improve Their Cytocompatibility and Reduce Inflammation Responses. *Colloids Surf., B* **2013**, *110*, 225–235.
- (5) Gristina, A. G. Biomaterial-Centered Infection: Microbial Adhesion Versus Tissue Integration. *Science* **1987**, *237*, 1588–1595.
- (6) Abbasi, F.; Mirzadeh, H.; Katbab, A. A. Modification of Polysiloxane Polymers for Biomedical Applications: A Review. *Polym. Int.* **2001**, *50*, 1279–1287.
- (7) Suchatlampong, C.; Davies, E.; von Fraunhofer, J. A. Frictional Characteristics of Resilient Lining Materials. *Dental Mater.* **1986**, *2*, 135–138.
- (8) Waters, M. G. J.; Jagger, R. G.; Polyzois, G. L. Wettability of Silicone Rubber Maxillofacial Prosthetic Materials. *J. Prosthet. Dent.* **1999**, *81*, 439–443.
- (9) Packham, D. E. Surface Roughness and Adhesion. In *Surfaces Chemistry and Applications*; Chaudhury, M. K., Pocius, A. V., Eds.; Elsevier: Amsterdam, The Netherlands, 2002; pp 317–350.
- (10) Okada, T.; Ikada, Y. Surface Modification of Silicone for Percutaneous Implantation. *J. Biomater. Sci., Polym. Ed.* **1995**, *7*, 171–180.
- (11) Lee, D.; Yang, S. Surface Modification of PDMS by Atmospheric-Pressure Plasma-Enhanced Chemical Vapor Deposition and Analysis of Long-Lasting Surface Hydrophilicity. *Sens. Actuators, B* **2012**, *162*, 425–435.
- (12) Tu, Q.; Wang, J. C.; Liu, R.; He, J.; Zhang, Y.; Shen, S.; Xu, J.; Liu, J.; Yuan, M. S.; Wang, J. Antifouling Properties of Poly(dimethylsiloxane) Surfaces Modified with Quaternized Poly(dimethylaminoethyl methacrylate). *Colloids Surf., B* **2013**, *102*, 361–370.
- (13) Gonçalves, S.; Leirós, A.; van Kooten, T.; Dourado, F.; Rodrigues, L. R. Physicochemical and Biological Evaluation of Poly(ethylene glycol) Methacrylate Grafted onto Poly(dimethylsiloxane) Surfaces for Prosthetic Devices. *Colloids Surf., B* **2013**, *109*, 228–235.
- (14) Daneshpour, N.; Collighan, R.; Perrie, Y.; Lambert, P.; Rathbone, D.; Lowry, D.; Griffin, M. Indwelling Catheters and Medical Implants with FXIIIa Inhibitors: A Novel Approach to the Treatment of Catheter and Medical Device-Related Infections. *Eur. J. Pharm. Biopharm.* **2013**, *83*, 106–113.
- (15) Chen, S. Y.; Chen, T. M.; Dai, N. T.; Fu, J. P.; Chang, S. C.; Deng, S. C.; Chen, S. G. Do Antibacterial-Coated Sutures Reduce

Wound Infection in Head and Neck Cancer Reconstruction? *Eur. J. Surg. Oncol.* **2011**, *37*, 300–304.

(16) Hetrick, E. M.; Schoenfisch, M. H. Reducing Implant-Related Infections: Active Release Strategies. *Chem. Soc. Rev.* **2006**, *35*, 780–789.

(17) Williams, D. L.; Haymond, B. S.; Beck, J. P.; Savage, P. B.; Chaudhary, V.; Epperson, R. T.; Kawaguchi, B.; Bloebaum, R. D. In Vivo Efficacy of a Silicone-Cationic Steroid Antimicrobial Coating to Prevent Implant-Related Infection. *Biomaterials* **2012**, *33*, 8641–8656.

(18) Lim, K.; Chua, R. R. Y.; Saravanan, R.; Basu, A.; Mishra, B.; Tambyah, P. A.; Ho, B.; Leong, S. S. J. Immobilization Studies of an Engineered Arginine–Tryptophan-Rich Peptide on a Silicone Surface with Antimicrobial and Antibiofilm Activity. *ACS Appl. Mater. Interfaces* **2013**, *5*, 6412–6422.

(19) Poelstra, K. A.; Barekzi, N. A.; Rediske, A. M.; Felts, A. G.; Slunt, J. B.; Grainger, D. W. Prophylactic Treatment of Gram-Positive and Gram-Negative Abdominal Implant Infections Using Locally Delivered Polyclonal Antibodies. *J. Biomed. Mater. Res.* **2002**, *60*, 206–215.

(20) Soulas, D. N.; Papadokostaki, K. G.; Panou, A.; Sanopoulou, M. Drug Release from Poly(dimethylsiloxane)-Based Matrices: Observed and Predicted Stabilization of the Release Rate by Three-Layer Devices. *Ind. Eng. Chem. Res.* **2012**, *51*, 7126–7136.

(21) Karami, S.; Imani, M.; Farahmandghavi, F. A novel image analysis approach for evaluation of mixing uniformity in drug-filled silicone rubber matrix. *Int. J. Pharm.* **2014**, *460*, 158–164.

(22) Forbes, C. J.; McCoy, C. F.; Murphy, D. J.; Woolfson, A. D.; Moore, J. P.; Evans, A.; Shattock, R. J.; Karl Malcolm, R. Modified silicone elastomer vaginal gels for sustained release of antiretroviral HIV microbicides. *J. Pharm. Sci.* **2014**, *103*, 1422–1432.

(23) Woolfson, A. D.; Elliott, G. R. E.; Gilligan, C. A.; Passmore, C. M. Design of an intravaginal ring for the controlled delivery of 17 β -estradiol as its 3-acetate ester. *J. Controlled Release* **1999**, *61*, 319–328.

(24) Woolfson, A. D.; Malcolm, R. K.; Gallagher, R. J. Design of a silicone reservoir intravaginal ring for the delivery of oxybutynin. *J. Controlled Release* **2003**, *91*, 465–476.

(25) Malcolm, R. K.; McCullagh, S. D.; Woolfson, A. D.; Gorman, S. P.; Jones, D. S.; Cuddy, J. Controlled release of a model antibacterial drug from a novel self-lubricating silicone biomaterial. *J. Controlled Release* **2004**, *97*, 313–320.

(26) Algeri, C.; Drioli, E.; Donato, L. Development of mixed matrix membranes for controlled release of ibuprofen. *J. Appl. Polym. Sci.* **2013**, *128* (1), 754–760.

(27) Suwannateep, N.; Banlunara, W.; Wanichwecharungruang, S. P.; Chiablaem, K.; Lirdprapamongkol, K.; Svasti, J. Mucoadhesive Curcumin Nanospheres: Biological Activity, Adhesion to Stomach Mucosa and Release of Curcumin into the Circulation. *J. Controlled Release* **2011**, *151*, 176–182.

(28) Roth, J.; Albrecht, V.; Nitschke, M.; Bellmann, C.; Simon, F.; Zschoche, S.; Michel, S.; Luhmann, C.; Grundke, K.; Voit, B. Surface Functionalization of Silicone Rubber for Permanent Adhesion Improvement. *Langmuir* **2008**, *24*, 12603–12611.

(29) De Givenchy, E. P. T.; Amigoni, S.; Martin, C.; Andrada, G.; Caillier, L.; G ribaldi, S.; Guittard, F. Fabrication of Superhydrophobic PDMS Surfaces by Combining Acidic Treatment and Perfluorinated Monolayers. *Langmuir* **2009**, *25*, 6448–6453.

(30) Wangthong, S.; Palaga, T.; Rengpipat, S.; Wanichwecharungruang, S. P.; Chanchaisak, P.; Heinrich, M. Biological Activities and Safety of Thanaka (*Hesperethusa Crenulata*) Stem Bark. *J. Ethnopharmacol.* **2010**, *132*, 466–472.

(31) Kidsaneepoiboon, P.; Wanichwecharungruang, S. P.; Choopawa, T.; Deephum, R.; Panyathanmaporn, T. Organic–Inorganic Hybrid Polysilsesquioxane Nanospheres as UVA/UVB Absorber and Fragrance Carrier. *J. Mater. Chem.* **2011**, *21*, 7922–7930.

(32) Richey, T.; Iwata, H.; Oowaki, H.; Uchida, E.; Matsuda, S.; Ikada, Y. Surface Modification of Polyethylene Balloon Catheters for Local Drug Delivery. *Biomaterials* **2000**, *21*, 1057–1065.

(33) Sansukharearnpon, A.; Wanichwecharungruang, S.; Leepipatpaiboon, N.; Kerdcharoen, T.; Arayachukeat, S. High Loading

Fragrance Encapsulation Based on a Polymer-Blend: Preparation and Release Behavior. *Int. J. Pharm.* **2010**, *391*, 267–273.

(34) Wattanasatcha, A.; Rengpipat, S.; Wanichwecharungruang, S. Thymol Nanospheres as an Effective Anti-Bacterial Agent. *Int. J. Pharm.* **2012**, *434*, 360–365.